Universal Critical Dynamics in High Resolution Neuronal Avalanche Data

Nir Friedman,[1] Shinya Ito,[2] Braden A. W. Brinkman,[1] Masanori Shimono,[2,5] R. E. Lee DeVille,[3] Karin A. Dahmen,[1] John M. Beggs,[2] and Thomas C. Butler[4,*]

[1]*Department of Physics, University of Illinois at Urbana-Champaign, 1110 West Green Street, Urbana, Illinois 61801, USA*
[2]*Department of Physics, Indiana University, 727 East Third Street, Bloomington, Indiana 47405, USA*
[3]*Department of Mathematics, University of Illinois at Urbana-Champaign, 1409 West Green Street, Urbana, Illinois 61801, USA*
[4]*Department of Physics, Massachusetts Institute of Technology, 77 Massachusetts Avenue, Cambridge, Massachusetts 02139, USA*
[5]*Graduate School of Education, The University of Tokyo, 7-3-1 Hongo, Bunkyo-ku, Tokyo 113-0033, Japan*

(Received 8 December 2011; revised manuscript received 27 February 2012; published 16 May 2012)

The tasks of neural computation are remarkably diverse. To function optimally, neuronal networks have been hypothesized to operate near a nonequilibrium critical point. However, experimental evidence for critical dynamics has been inconclusive. Here, we show that the dynamics of cultured cortical networks are critical. We analyze neuronal network data collected at the individual neuron level using the framework of nonequilibrium phase transitions. Among the most striking predictions confirmed is that the mean temporal profiles of avalanches of widely varying durations are quantitatively described by a single universal scaling function. We also show that the data have three additional features predicted by critical phenomena: approximate power law distributions of avalanche sizes and durations, samples in subcritical and supercritical phases, and scaling laws between anomalous exponents.

DOI: 10.1103/PhysRevLett.108.208102 PACS numbers: 87.19.lj, 64.60.aq, 64.60.av, 87.19.ll

The notion of an avalanche flows naturally from the basic operation of the brain's network. Neurons influence the firing of other neurons through a network of axons, synapses, and dendrites [1]. These connections allow neuronal firing to propagate, leading to avalanches of activity [2]. Like avalanches seen in physical systems such as earthquakes, nanocrystals, and magnets, the sizes of neuronal avalanches are typically power law distributed [2–5]. In condensed matter systems, the power law distribution of avalanche sizes has been explained by use of the theory of critical phenomena associated with phase transitions [4]. While power law distributions of neuronal avalanches suggest that neuronal networks may also operate near a critical point, this hypothesis is controversial due to the many possible mechanisms of generating power law distributions and the limited resolution of available experimental data [6–10].

Here, we go beyond power law analysis by demonstrating that data from high-resolution measurements of cultured cortical slices taken from rats show the emergence of quantitative universal avalanche dynamics across many scales. These universal dynamics are found by analyzing the mean temporal profiles of the experimentally measured avalanches over a wide range of durations. Standard rescaling of the axes according to theory with no adjustable parameters collapses the data and yields a single universal scaling function [4]. The emergence of universality demonstrated by data collapse is among the most striking and generic predictions of criticality and is much less subject to a multiplicity of explanations than power law analysis alone [4,11–13]. Additional characteristics of systems near criticality include relations between scaling exponents and two distinct phases on both sides of the critical point, which were also present in our data. We emphasize that in addition to confirming the presence of criticality, our results provide a highly detailed picture of neuronal avalanche dynamics.

To generate sufficiently high-resolution data, we removed 400 μm thick slices of cortical tissue from living rats, cultured them until they reached maturity (approximately one month), and placed them on an array of 512 electrodes spaced 60 μm apart as shown in Fig. 1(a) [see Supplemental Material (SM) [14]] [15]. Our array allowed us to generate time series of voltage spikes (firing events) from 100–340 individual neurons at a spacing where synaptic connections are relatively likely [see Figs. 1(b)–1(d)] [16]. From this data we resolved avalanches of firing events [Figs. 1(e) and 1(f)]. For further details, see SM [14]. In contrast, previous work used arrays with electrode spacings of 200–500 μm limiting data collection to either widely spaced neurons [17] or to lower resolution local field potential (LFP) data [2,18]. LFP data convolve all electrical activity over a wide area. This convolution, combined with the fact that related analyses are usually limited to seeking power laws, makes drawing conclusions about criticality difficult [6–10].

Analysis of the avalanche data indicates that like many avalanching systems, cortical tissues can be in one of two phases: one in which the avalanches are small and die out quickly, and another in which avalanches are large and tend to span the size of the system. Between these two phases there is a critical point, where the distribution of avalanche sizes follows a power law. The renormalization group predicts that the dynamics near the critical point have

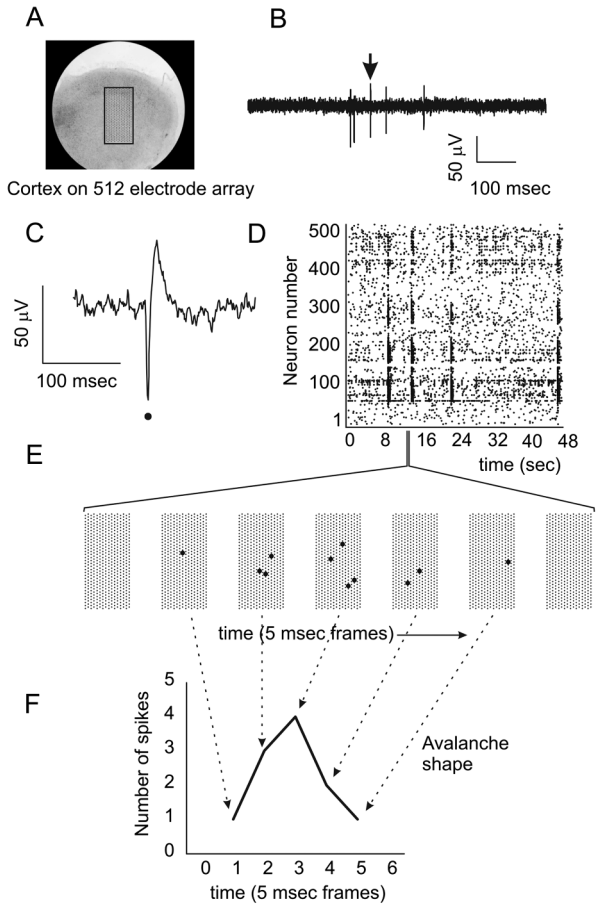

FIG. 1. Recording avalanches from cortical tissue. (a) Micrograph of cultured cortical slice on a 512 electrode array. Black rectangle (1 mm × 2 mm) added to highlight location of array. (b) Voltage trace from one electrode. Arrow marks a spike from an individual neuron, expanded in (c). Time of spike is marked by black dot. (d) Raster plot of spike times (dots) from many neurons over a 48 s interval. Recordings lasted up to 8 h. (e) Expanded view of network activity reveals an avalanche. Each frame represents the array at one 5 ms bin. Small dots are electrode locations; large dots are spikes on array. An avalanche consists of consecutively active frames, bracketed by inactive frames, as shown here. (f) Avalanche shape is obtained by plotting the number of spikes in each frame versus time.

universal (i.e., detail independent) scale-invariant properties [4]. The independence from microscopic details implies that an appropriate simple model will capture the universal dynamics near the critical point.

To probe the universality class, we use a modified version of the discrete time-step model studied by DeVille *et al.* [19,20] (see SM [14]). At any time step each of the N neurons in the system is either firing or not firing. If neuron i fires at time t, then it has probability p_{ij} to trigger neuron j to fire at time $t + 1$. Here we use transfer entropy techniques to extract all triggering probabilities p_{ij} for each experimental sample (see SM [14]). These probabilities are then built into the model simulations so that for each experiment we have a corresponding set of triggering probabilities and simulation results.

The data taken from both experiment and simulation are structured as a collection of time series of firing activity, one per neuron. In both cases an avalanche is defined by a consecutive sequence of time steps for which there is firing activity, bounded before and after by a time interval of zero activity [see Figs. 1(d)–1(f)]. Each avalanche has a corresponding duration (number of time steps with uninterrupted activity), size (total number of neurons that fired during the avalanche), and temporal profile or shape (a plot of the number of neurons that fire in each time step during the avalanche).

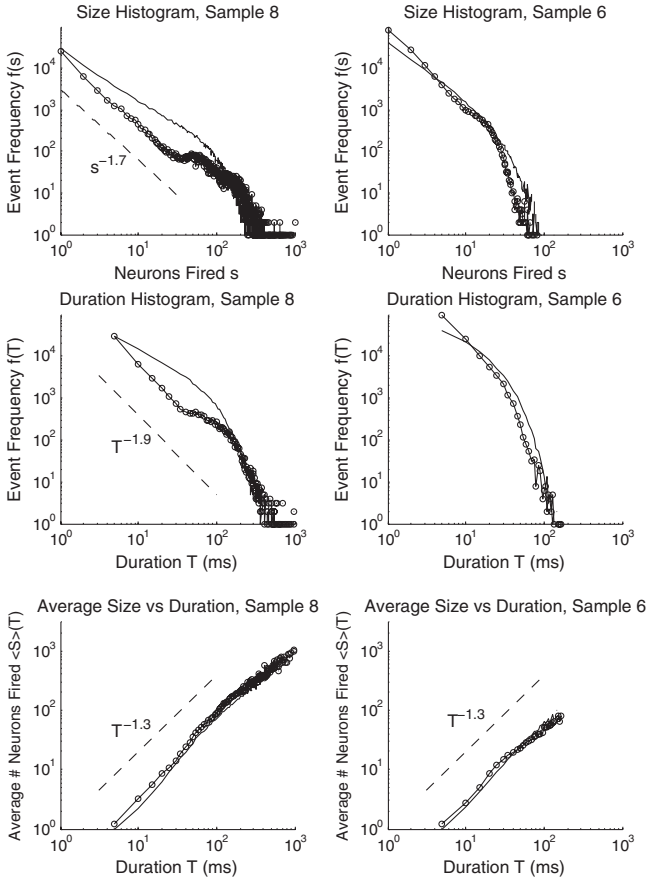

FIG. 2. Contrasting size and duration distributions and average size for fixed duration from a critical data set (left) and a subcritical data set (right). Experimental data are shown by lines with markers and data from the corresponding models are shown by smooth lines. Note that each experimental data set has its own simulation as we use information from the experiment to determine the parameters of the simulation (see SM [14]). The dashed lines on the left (near critical) column correspond to power laws with exponent 1.7, 1.9, and 1.3, corresponding to the critical exponents τ, α, and $1/\sigma\nu z$, respectively. These values satisfy the exponent relation $\frac{\alpha-1}{\tau-1} = \frac{1}{\sigma\nu z}$, as is expected for a system near criticality. Statistical error bars are only significant for the largest and longest events for the experimental data and are too small to see in the figure for the simulations.

Histograms of avalanche sizes and durations from experiments and simulations are shown in Fig. 2. Scaling theory predicts the functional forms for these distributions near a critical point:

$$f(S) \sim S^{-\tau} \tag{1}$$

$$f(T) \sim T^{-\alpha} \tag{2}$$

$$\langle S \rangle(T) \sim T^{1/\sigma\nu z}, \tag{3}$$

where f is the probability density function of the associated variable, S is the size of a neuronal avalanche, T is the duration, and $\langle S \rangle(T)$ is the average size conditioned on a given duration [4]. The parameters τ, α, and $1/\sigma\nu z$ are critical exponents of the system and are expected to be independent of the details of the system or model, i.e., to be the same for all systems in the same universality class [4]. These forms are valid near criticality for intermediate length and time scales [4], although what constitutes ''near'' can vary from exponent to exponent. For example, relation (3) above is valid quite far from criticality.

For some experiments, the power law region of the avalanche size distributions spans two decades (Fig. 2), which is the largest range that can be expected for experiments that track on the order of 100 neurons. This range of scaling is comparable to cutting edge work on avalanching critical points in condensed matter systems [13].

For the two critical data sets, we found the following exponents: $\tau = 1.6 \pm 0.2$, $\alpha = 1.7 \pm 0.2$, and $1/\sigma\nu z = 1.3 \pm 0.05$. Consistent, well-defined, critical exponents are only expected near criticality. To study the origin of the best characterized exponent, $1/\sigma\nu z$, we simulated the neuronal network under different sets of assumptions. Possible factors affecting the value of $1/\sigma\nu z$ include network structure as encapsulated in p_{ij}, as well as other key physiological properties of neurons such as a refractory period for the neurons and storage of electrochemical potential. Simulations with refractory periods and stored electrochemical potential added to the model whose network structure was all-to-all failed to reproduce the exponent. In contrast, in simulations with network structures that were given by the appropriate p_{ij} drawn from experiments, the model predicts the same value for $1/\sigma\nu z$ (1.3) as obtained in experiments. It also captures qualitatively the form of the size and duration distributions. Thus, the simulation results are satisfactory, considering the remarkable simplicity of the model. If p_{ij} is a constant p for all pairs of neurons, $1/\sigma\nu z = 2.0$. The sensitivity of the scaling exponents to the matrix p_{ij} clearly indicates that the structure of the network qualitatively affects the

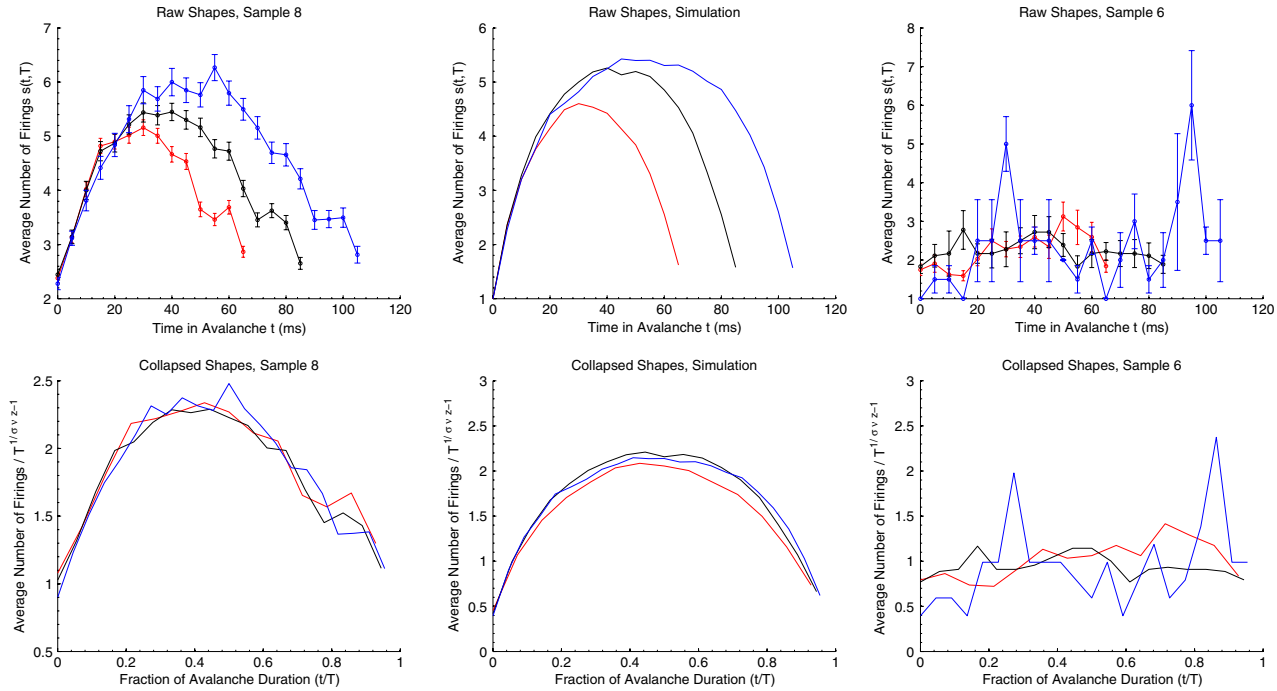

FIG. 3 (color online). Avalanche shape collapses. Shapes and attempted collapses from three data sets: two experimental and one simulated. Shapes are produced by averaging the temporal profiles of all avalanches of a particular duration; different colors here represent different durations. The collapses are plotted by rescaling the horizontal and vertical axes. The left- and rightmost data correspond to experimental data close to and far from criticality, respectively (note these are the same data sets used in Fig. 2). Sample 8 clearly shows the roughly parabolic shapes in the raw data and a corresponding very clean collapse, as would be expected from critical data. Sample 6 shows neither. The middle plots are a simulation of sample 8, using transfer entropy data from that set [14]. They clearly show similar shapes and collapse to a universal scaling function.

critical dynamics and is the primary factor determining the value of $1/\sigma\nu z$.

Scaling theory also predicts exponent relations. In particular, the above three exponents are related as [4]

$$\frac{\alpha - 1}{\tau - 1} = \frac{1}{\sigma\nu z}. \quad (4)$$

The experimental exponent values in the critical sample shown in Fig. 2 (left column) are consistent with this relation.

One of the most stringent predictions of the theory of dynamic critical phenomena is that the mean temporal profile of avalanches is universal across scales (data collapse). For avalanches of duration T we can write down the average number of neurons firing, s, at time t as

$$s(t, T) \sim T^{1/\sigma\nu z - 1}\mathcal{F}(t/T), \quad (5)$$

where $\mathcal{F}$ is a universal scaling function that determines the shape of the average temporal profile. $\langle S\rangle(T)$ and $s(t, T)$ are related by $\langle S\rangle(T) = \int_0^T s(t, T)dt$. Since a function has infinitely more degrees of freedom than a single number, scaling functions contain more information than scaling exponents, and collapses fail faster as one moves away from criticality. Near the critical point, plots of t/T versus $s(t, T)T^{1-1/\sigma\nu z}$ for different T will collapse onto the same universal scaling function, $\mathcal{F}$.

The two critical data sets collapse extremely well to scaling functions $\mathcal{F}$ while the other eight data sets do not. Figure 3 shows avalanche shapes for avalanches with three different durations. We fit the scaling functions using a set of orthonormal polynomials [5] and found that the functions are very close to parabolas as predicted by mean field theory, in contrast to experiments in other systems where large asymmetries or flattening are present [5,13]. Each shape collapse contains data from tens of thousands of points and is not a statistical artifact, as shuffled data sets do not collapse (see SM [14]).

The other eight data sets are in either subcritical or supercritical phases. That cultured samples can take on a range of noncritical behavior (Fig. 4) has been suspected from LFP data and has even been controlled by the use of drugs [2,21,22]. Both network topology and connection strength influence the phase of a given sample. Increasing the number or the strength of connections in a network moves the network toward supercriticality (see SM [14] for example) consistent with simulation results [19]. Based on the histograms, exponent relations, and data collapse, it appears that sample 8 is close to the critical point while sample 6 is subcritical. Our findings are consistent with cultured experiments showing that networks slowly pass through subcritical, supercritical, and critical phases over weeks of development [23]. For mature cortical tissue, departures from criticality may correspond to pathological states. Recent studies suggest that epilepsy is one such state [24].

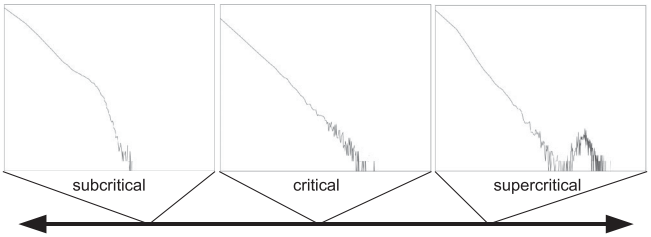

FIG. 4. Avalanche size histograms from three different samples of rat cortex. The horizontal line represents a path in some representative (such as increasing mean connection strength or increasing number of connections) direction in the complex parameter space of network, representing how critical the sample of interest is. As we move along this path towards greater network connectivity, samples change from having early exponential cutoffs, to straightforward power laws, to having humps in their distribution. These humps could be caused by the possibility that the finite system size, rather than the degree of network connection, is constraining the size of the largest events. These histograms show that different samples exist at different points in the phase diagram, such as the mean connection strength with fixed network topology, toward increasing excitability. Factors that determine the phase of a given sample include number of connections and connection strength. Simulations using a mean field (all-to-all connectivity) version of our model can move along the phase diagram by increasing connection strength [19,20]. Experiments have used drugs to move the network along this line in the parameter space [2,21,22].

The above analysis focused on high resolution measurements of organotypic cortical cultures. Use of these cultures allowed us to analyze the activity of large numbers of individual neurons and obtain detailed information about the shapes of avalanches and their scaling (see Fig. 3). The neuronal networks in cortical cultures are thought to capture many of the gross patterns of connectivity found in intact brains [25], suggesting that our results may be relevant for intact brains. Experiments using lower resolution local field potential measurements on intact brains have succeeded in demonstrating power law avalanche size and duration distributions [18] but have not succeeded in demonstrating shape collapse. We also analyzed data from 10 dissociated cultures of cortical neurons, where connectivity is known to substantially differ from organotypic cultures [26]. While data from dissociated cultures contained far fewer neurons (~ 40) than in the organotypic data sets, we observed approximate shape collapse for seven samples, but with different critical exponents than those observed in organotypic samples (see SM [14] for representative collapse).

Power law histograms of avalanches in local field potential data have long been suggestive of nonequilibrium critical behavior, but are not sufficient evidence of criticality. By collecting signals resolved for closely spaced individual neurons and extracting universal scaling exponents and functions, we provide compelling evidence that networks of cultured cortical neurons can operate near a

critical point. In contrast to condensed matter and geological systems, criticality in cortical tissue has additional significance through its relation to optimal information processing, information storage, dynamic response, and computation [2,21,22,27–30]. The collapse of avalanche data onto a universal scaling function as predicted by the theory of dynamic critical phenomena provides a clear demonstration of quantitative universality in a biological system [31–34]. The success of a simple model utilizing a complex, empirically determined network shows that the critical dynamics depend intricately on a unique network structure. Finally, the existence of both critical and noncritical samples and a criterion for distinguishing them opens the door for precise experimental tests of the hypothesis that critical neuronal networks function optimally.

We thank Alan Litke, Nigel Goldenfeld, Jonathan Uhl, Andrew Ferguson, Gerardo Ortiz, and Eshel Ben-Jacob for helpful discussions. We acknowledge the financial support of a Post Graduate Scholarship from the Natural Sciences and Engineering Research Council of Canada (N. F., B. B.), National Science Foundation (NSF) Physics Frontier Center Grant No. 0822613 Center for the Physics of the Living Cell (N. F.), NSF Grants No. POLS-1058291 and No. CRCNS-0904912 (J. M. B.), NSF Grant No. DMR-1005209 (K. A. D.), JSPS Research Fellowships for Young Scientists (M. S.), and NSF Grant No. CMG-0934491 (R. E. L. D.).

*To whom correspondence should be addressed.
tbutler@mit.edu

[1] Tim P. Vogels, Kanaka Rajan, and L. F. Abbott, Annu. Rev. Neurosci. **28**, 357 (2005).
[2] John M. Beggs and Dietmar Plenz, J. Neurosci. **23**, 11 167 (2003) [http://www.jneurosci.org/content/23/35/11167.short].
[3] Dennis M. Dimiduk, Chris Woodward, Richard LeSar, and Michael D. Uchic, Science **312**, 1188 (2006).
[4] James P. Sethna, Karin A. Dahmen, and Christopher R. Myers, Nature (London) **410**, 242 (2001).
[5] Amit P. Mehta, Andrea C. Mills, Karin A. Dahmen, and James P. Sethna, Phys. Rev. E **65**, 046139 (2002).
[6] C. Bédard, H. Kröger, and A. Destexhe, Phys. Rev. Lett. **97**, 118102 (2006).
[7] Viola Priesemann, Matthias Munk, and Michael Wibral, BMC Neurosci. **10**, 40 (2009).
[8] Jonathan Touboul and Alain Destexhe, PLoS ONE **5**, e8982 (2010).
[9] M. E. J. Newman, Contemp. Phys. **46**, 323 (2005).
[10] W. J. Reed and B. D. Hughes, Phys. Rev. E **66**, 067103 (2002).
[11] Nigel D. Goldenfeld, *Lectures on Phase Transitions and the Renormalisation Group* (Westview Press, New York, 1992).
[12] B. Widom, J. Chem. Phys. **43**, 3898 (1965).
[13] Stefanos Papanikolaou, Felipe Bohn, Rubem Luis Sommer, Gianfranco Durin, Stefano Zapperi, and James P. Sethna, Nature Phys. **7**, 316 (2011).
[14] See Supplemental Material at http://link.aps.org/supplemental/10.1103/PhysRevLett.108.208102 for details of experiments, modeling, robustness tests, and network reconstruction.
[15] Aonan Tang, David Jackson, Jon Hobbs, Wei Chen, Jodi L. Smith, Hema Patel, Anita Prieto, Dumitru Petrusca, Matthew I. Grivich, Alexander Sher, Pawel Hottowy, Wladyslaw Dabrowski, Alan M. Litke, and John M. Beggs, J. Neurosci. **28**, 505 (2008).
[16] Sen Song, Per Jesper Sjöström, Reigl Markus, Sacha Nelson, and Dmitri B. Chklovskii, PLoS Biol. **3**, e68 (2005).
[17] Tiago L. Ribeiro, Mauro Copelli, Fábio Caixeta, Hindiael Belchior, Dante R. Chialvo, Miguel A. L. Nicolelis, and Sidarta Ribeiro, PLoS ONE **5**, e14129 (2010).
[18] Thomas Petermann, Tara C. Thiagarajan, Mikhail A. Lebedev, Miguel A. L. Nicolelis, Dante R. Chialvo, and Dietmar Plenz, Proc. Natl. Acad. Sci. U.S.A. **106**, 15921 (2009).
[19] R. E. Lee DeVille and Charles S. Peskin, Bull. Math. Biol. **70**, 1608 (2008).
[20] R. E. Lee DeVille, Charles S. Peskin, and Joel H. Spencer, Math. Mod. Nat. Phenom. **5**, 26 (2010).
[21] Woodrow L. Shew, Hongdian Yang, Thomas Petermann, Rajarshi Roy, and Dietmar Plenz, J. Neurosci. **29**, 15595 (2009).
[22] Woodrow L. Shew, Hongdian Yang, Shan Yu, Rajarshi Roy, and Dietmar Plenz, J. Neurosci. **31**, 55 (2011).
[23] Tetzlaff Christian, Samora Okujeni, Ulrich Egert, Florentin Wörgötter, and Markus Butz, PLoS Comput. Biol. **6**, e1001013 (2010).
[24] J. P. Hobbs, J. L. Smith, and J. M. Beggs, J. Clin. Neurophysiol. **27**, 380 (2010).
[25] J. Bolz, N. Novak, M. Götz, and T. Bonhoeffer, Nature (London) **346**, 359 (1990).
[26] M. Garofalo, T. Nieus, P. Massobrio, and S. Martinoia, PLoS ONE **4**, e6482 (2009).
[27] Clayton Haldeman and John M. Beggs, Phys. Rev. Lett. **94**, 058101 (2005).
[28] Nils Bertschinger and Thomas Natschläger, Neural Comput. **16**, 1413 (2004).
[29] Robert Legenstein and Wolfgang Maass, Neural Netw. **20**, 323 (2007).
[30] Osame Kinouchi and Mauro Copelli, Nature Phys. **2**, 348 (2006).
[31] A. Cavagna, A. Cimarelli, I. Giardina, G. Parisi, R. Santagati, F. Stefanini, and M. Viale, Proc. Natl. Acad. Sci. U.S.A. **107**, 11865 (2010).
[32] T. Mora, A. M. Walczak, W. Bialek, and C. G. Callan, Proc. Natl. Acad. Sci. U.S.A. **107**, 5405 (2010).
[33] Thierry Mora and William Bialek, J. Stat. Phys. **144**, 268 (2011).
[34] M. Nykter, N. D. Price, M. Aldana, S. A. Ramsey, S. A. Kauffman, L. E. Hood, O. Yli-Harja, and I. Shmulevich, Proc. Natl. Acad. Sci. U.S.A. **105**, 1897 (2008).